

Identified hadron production at high transverse momenta in $p + p$ collisions at $\sqrt{s_{NN}} = 200$ GeV in STAR

Yichun Xu^a
for the STAR Collaboration

Department of Modern Physics, University of Science and Technology of China, Hefei, Anhui 230026, China
Physics Department, Brookhaven National Laboratory, Upton, NY 11973, USA

Received: 30 September 2008 / Published online: 6 February 2009
© Springer-Verlag / Società Italiana di Fisica 2009

Abstract We report the transverse momentum (p_T) distributions for identified charged pions, protons and anti-protons using events triggered by high deposit energy in the Barrel Electro-Magnetic Calorimeter (BEMC) from $p + p$ collisions at $\sqrt{s_{NN}} = 200$ GeV. The spectra are measured around mid-rapidity ($|y| < 0.5$) over the range of $3 < p_T < 15$ GeV/c with particle identification (PID) by the relativistic ionization energy loss (rdE/dx) in the Time Projection Chamber (TPC) of the Solenoidal Tracker at RHIC (STAR). The charged pion, proton and anti-proton spectra at high p_T are compared with published results from minimum bias triggered events and the Next-Leading-Order perturbative quantum chromodynamic (NLO pQCD) calculations (DSS, KKP and AKK 2008). In addition, we present the particle ratios of π^-/π^+ , \bar{p}/p , p/π^+ and \bar{p}/π^- in $p + p$ collisions.

PACS 12.38.Bx · 13.85.Ni

1 Introduction

The study of identified hadrons (π^\pm , K^\pm , $p(\bar{p})$) spectra at high p_T in $p + p$ collisions provides a good test of perturbative quantum chromodynamics (pQCD) [1–5]. In different NLO pQCD calculations, the inclusive production of single hadron is described by the convolution of parton distribution functions (PDFs), parton interaction cross-sections, and fragmentation functions (FFs) which are parameterized by measured hadron spectra. From the minimum-bias triggered $p + p$ collisions in the year 2003, the $p(\bar{p})$ and charged pion spectra were measured at $p_T \leq 7$ GeV/c and $p_T \leq 10$ GeV/c with significant systematic errors due to the uncertainties in mean dE/dx position for protons and

kaons [6]. In order to understand mechanism of hadron production, it is necessary to make a strict constraint on the quark and gluon FFs by comparing theory with experimental data. In addition, it's also a good baseline for studying color charge effect of parton energy loss in heavy ion collisions, in which hadron spectra were measured up to 12 GeV/c [7, 8].

In this article, we present the p_T spectra for identified charge pions, protons and anti-protons in $p + p$ collisions at $\sqrt{s_{NN}} = 200$ GeV by the STAR experiment at RHIC. The results will be compared with NLO pQCD calculations. The particle ratios of π^-/π^+ , \bar{p}/p , p/π^+ and \bar{p}/π^- in $p + p$ collisions will be presented and compared with results in $d + Au$ collisions [6, 9].

2 Experiment and analysis

The STAR main tracking detector, the TPC, covering full azimuthal angle (2π) and $|\eta| < 1.3$ in pseudo-rapidity provides a way to identify charged hadrons by measuring momentum and dE/dx information of charged particles. In addition, the BEMC covering 2π azimuthal angle and $0 < \eta < 1$ in year 2005 provides deposited energy of electron, and electro-magnetic shower shape, size and position, which are used to enhance electron yields relative to other hadrons. This is helpful for re-calibrating rdE/dx [10], which will be discussed later.

Due to empirical parameters in theory, gas multiplication gains and noise of the TPC electronics, and pileup in high luminosity environment, measured rdE/dx values are deviated from theoretical predictions. Dominant pion yields shadow kaons and protons in the rdE/dx distribution, although the rdE/dx separations among π^\pm , K^\pm , and $p(\bar{p})$ are about $1\text{--}3\sigma$. This results in large systematic errors due to the uncertainty of rdE/dx positions. Knowledge of the precise rdE/dx position for those hadrons is

^a e-mail: xuyichun@rcf.rhic.bnl.gov

important to understand the efficiencies of particle identification (PID) selection and to reduce the systematic uncertainty in identified hadron yields. In order to improve the PID at high p_T , the re-calibration method [10] is used to locate the rdE/dx positions for different charged particles with good precision. To separate pion and electron clearly and get rdE/dx of electron precisely, information of the BEMC is used to get electron enhancement data sample. Meanwhile, Strange hadrons $\Lambda \rightarrow p + \pi^-$ ($\bar{\Lambda} \rightarrow \bar{p} + \pi^+$) and $K_S^0 \rightarrow \pi^+ + \pi^-$ are reconstructed by their decay topology to identify their decay daughters in the TPC. This provides rdE/dx peak position from samples of pure protons and charged pions [10].

With these precise rdE/dx information, the left panel of Fig. 2.1 shows the deviation of rdE/dx normalized by pion rdE/dx between data and theoretical values. This distribution is described by a function, $f(x) = A + \frac{B}{C+x^2}$. Meanwhile, the separation between identified hadrons and pions are derived from this fit function, as shown on the right panel of Fig. 2.1.

In order to extract charged pion and proton (anti-proton) yields, a total of 5.6 million BEMC triggered events in year 2005 (with transverse energy $E_T > 6.4$ GeV) have been analyzed. The details of BEMC trigger condition can be found in Ref. [11]. Since pions are the dominant component of the hadrons, pion raw yields can be derived by fitting rdE/dx distribution using 8-Gaussian with four fixed re-calibrated parameters for peak positions. The left panel of Fig. 2.2 shows the rdE/dx distribution at $5.0 < p_T < 5.5$ GeV/c and $|\eta| < 0.5$. For proton yields, we used two methods. One method is based on track-by-track selection using a cut in rdE/dx . The other method is fitting dE/dx distribution with fixed proton peak position. The final yields we used

in this analysis are averaged from these two methods. Half of the difference (<13%) between them is included in systematic uncertainty.

The right panel on Fig. 2.2 shows that there is great difference between invariant yields of charged pions from BEMC triggered events (red and blue circles) and minimum bias events (black squares) because of trigger enhancement. In order to correct this effect, PYTHIA events are embedded in GEANT with STAR geometry, which can simulate the realistic response of the STAR detector in experiment, including signal of read-out and response of electronics, when tracks are propagated through detectors. With simulated signal, different triggered events are selected by passing different detector thresholds as real events in STAR experiment. On the right panel in Fig. 2.2, stars and triangles represent charged pion spectra from simulated BEMC triggered and minimum bias events.

With the simulation, we can calculate the enhancement factors versus p_T by dividing BEMC triggered spectra by minimum bias triggered spectra. With the trigger enhancement factors and tracking efficiencies (~88% at $3 < p_T < 15$ GeV/c), the charged pion spectra are corrected and shown on the left panel of Fig. 2.3. The corrected spectra of pions are consistent with minimum bias results at the overlapped p_T range, and the NLO pQCD calculations. With p/π^+ and \bar{p}/π^- ratios, the invariant yields of proton (anti-proton) are calculated by pion spectra times p/π^+ (\bar{p}/π^-) ratios. The spectra of protons and anti-protons are shown on the right panel in Fig. 2.3. Almost all these NLO pQCD predictions can not describe our proton and anti-proton spectra well at high p_T , especially AKK 2008 for anti-proton, which is going down to zero at 9 GeV/c (from S. Albino private communication). The

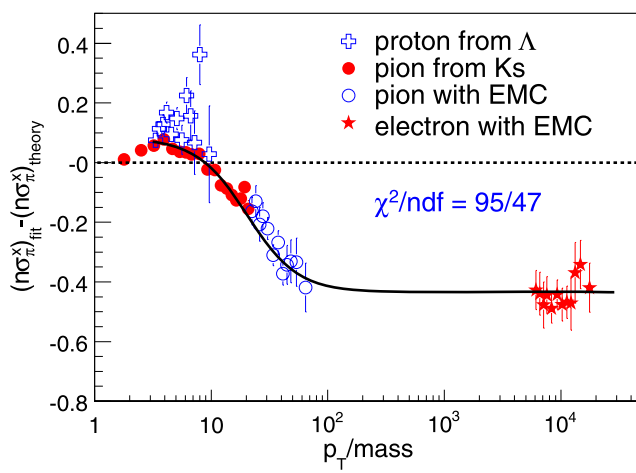
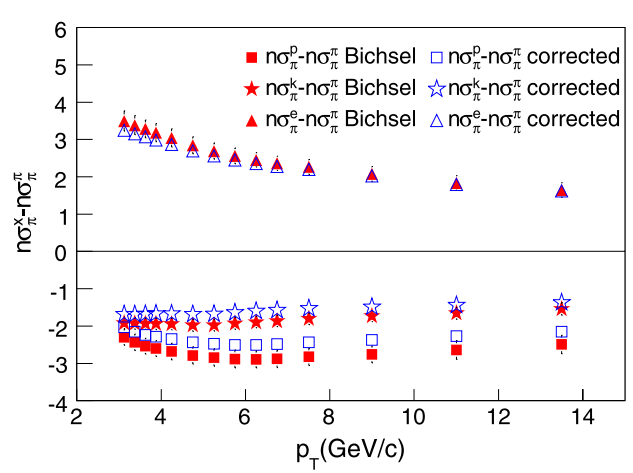


Fig. 2.1 (Color online) On the left panel, the dE/dx deviation in σ as functions of transverse momentum divided by mass (p_T/mass). The blue crosses are proton decayed from Λ , the red filled dots are pion from K_S^0 , and blue open circles and red stars are pion and electron from



electronenhancement sample respectively. On the right panel, comparison of the relative dE/dx peak position of $n\sigma_\pi^K$, $n\sigma_\pi^p$, $n\sigma_\pi^e$. All solid dots depict theoretical values, and open ones are re-calibrated results

AKK 2008 [12] includes BRAHMS data points at high rapidity ($2.95 < y < 3.1$) [13] for parametrization. Our data will provide a good constraint for the NLO pQCD calculation.

The total systematic uncertainties associated with pion are estimated to be less than 15%. The systematic uncertainty consists of uncertainty of peak position (<4%), charge distortion (<12%), momentum resolution (<5%) and efficiencies (<5%). Proton spectra have similar systematic uncertainty sources. In addition, two methods to getting proton yields results in $\sim 13\%$ contribution.

The particle ratios at mid-rapidity as a function of p_T are shown on Fig. 2.4, and compared with published results from minimum bias $p + p$ and $d + Au$ collisions. The predictions from different model, such as PYTHIA, DSS, and AKK 2008 are also shown. All the boxes and

bars represent systematical and statistical errors. Our results are consistent with those from minimum bias $p + p$ collisions. For the models, only PYTHIA can describe these ratios well, DSS over-predicts anti-proton, AKK 2008 over-predicts proton, and under-predicts anti-proton. The π^-/π^+ ratio from BEMC triggered events decreases with increasing p_T , which indicates significant valence quark contribution to charge pion production. The decrease of \bar{p}/p ratio also indicates a significant quark contribution to baryon production. The p/π^+ and \bar{p}/π^- ratios decrease at intermediate p_T range ($2 < p_T < 6$ GeV/c) and approach constant at high p_T , which are consistent with PYTHIA simulation. The p/π^+ ratio in $p + p$ collision is lower than that in $d + Au$ collisions in the intermediate p_T range.

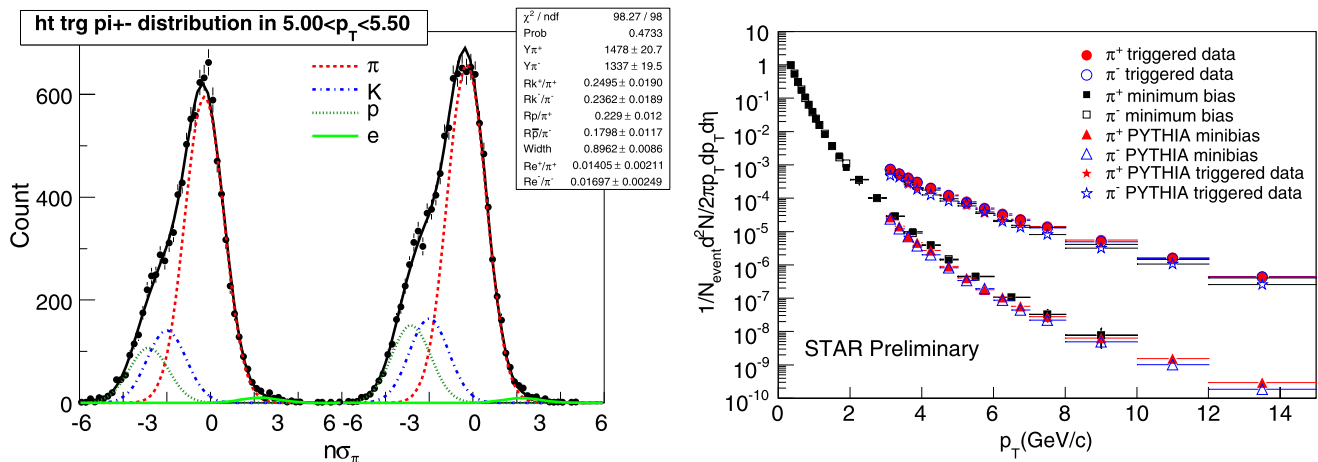


Fig. 2.2 (Color online) On the left panel, $n\sigma_\pi^h$ distribution at $3.75 < p_T < 4.0$ GeV/c for positive (right part) and negative (left part) particles. The black line is the fit curve by 8-Gaussian function, including pion (red dashed line), kaon (blue dot-dashed line), proton

(green dotted line), and electron (green solid line). On the right panel, pion spectra from minimum bias events, BEMC triggered events, and simulated minimum bias and BEMC triggered events

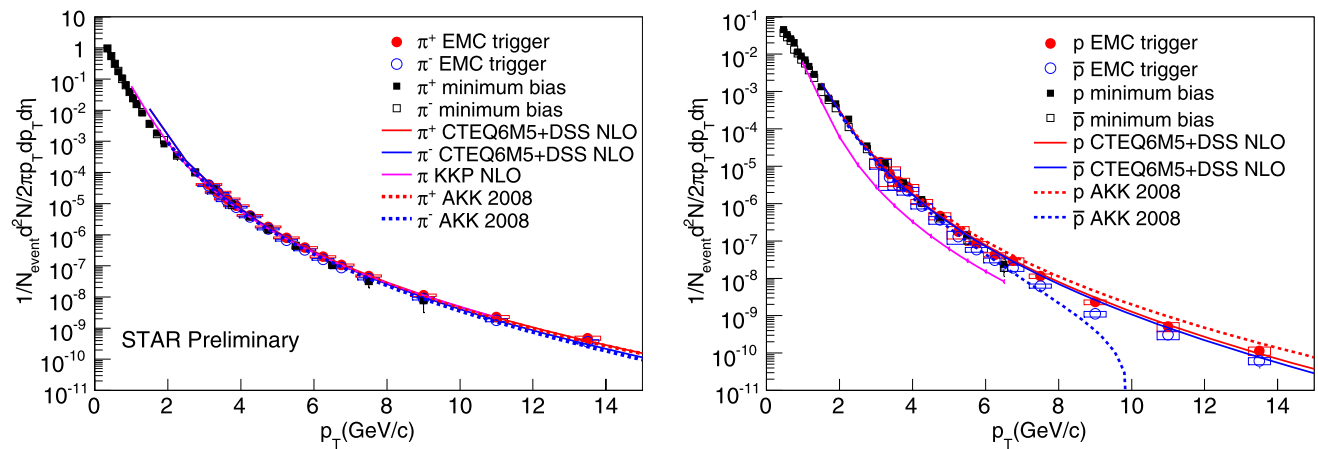


Fig. 2.3 (Color online) Spectra for pion (on the left panel) and proton (on the right panel) with NLO pQCD calculations including DSS, AKK 2008

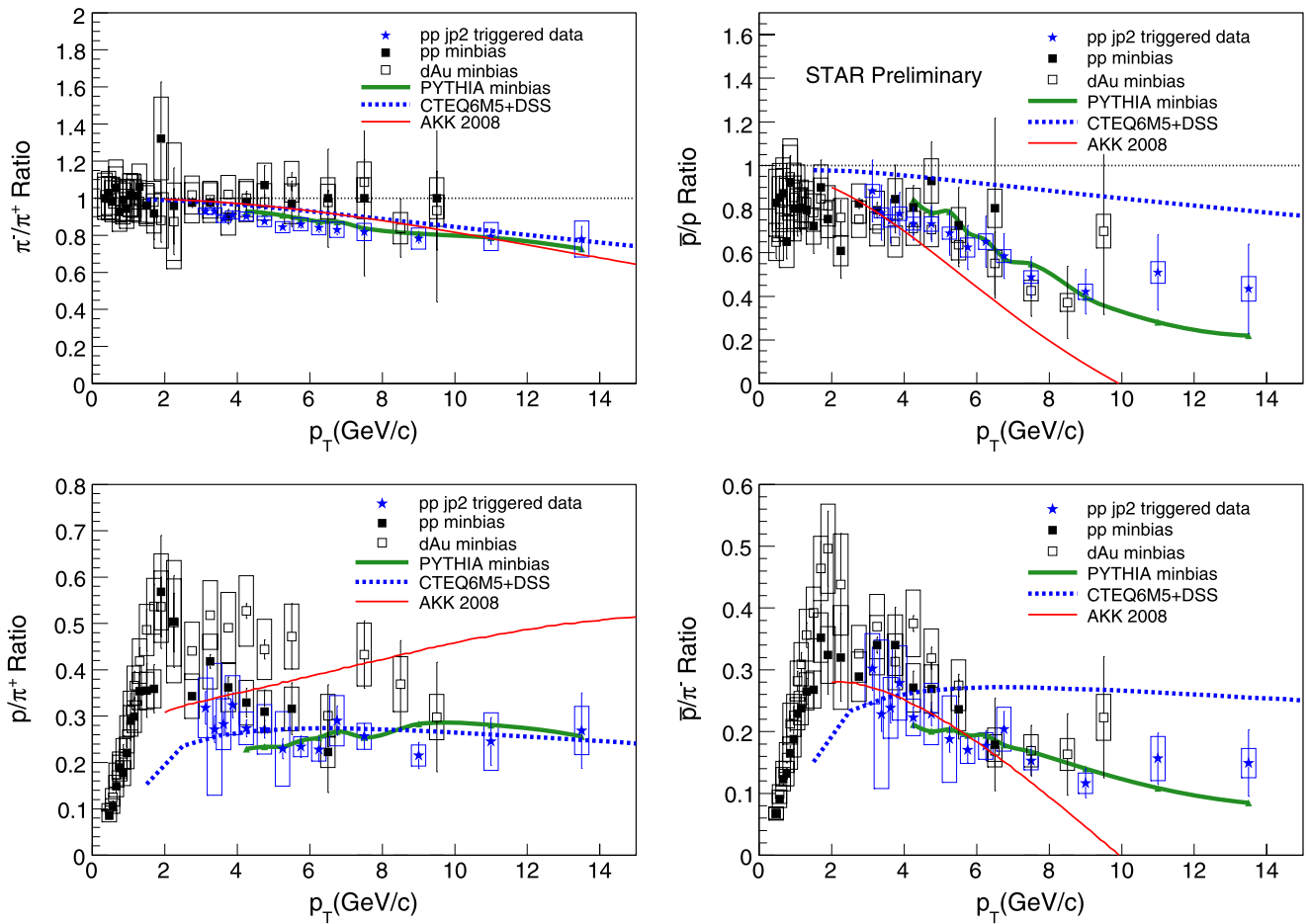


Fig. 2.4 (Color online) Ratios of π^-/π^+ , \bar{p}/p , p/π^+ and \bar{p}/π^- from minimum bias events (black squares), BEMC triggered events (blue stars), and PYTHIA simulation (green solid line), DSS (blue dashed-line) and AKK 2008 (red solid line) predictions

3 Summary and discussion

We have presented transverse momentum spectra for identified charged pions, protons and anti-protons from $p + p$ collisions triggered by the BEMC at $\sqrt{s_{NN}} = 200$ GeV. With PYTHIA and GEANT simulation, the transverse momentum spectra around mid-rapidity ($|\eta| < 0.5$) are extended up to $p_T > 15$ GeV/c with PID by the rdE/dx in the TPC. Comparison of spectra to NLO pQCD predictions, DSS and AKK 2008 shows a good agreement for pions spectra, but a poor one for proton and anti-proton spectra, especially AKK 2008 for anti-proton. Our data can provide a good constraint to the pQCD calculations, and furthermore, understand quark and gluon contributions. Ratios of π^-/π^+ , \bar{p}/p , p/π^+ and \bar{p}/π^- are consistent with PYTHIA, but inconsistent with NLO pQCD calculations, i.e. DSS over-predict anti-protons, AKK 2008 over-predict proton, and under-predict anti-proton. In addition, the decrease of π^-/π^+ and \bar{p}/p indicate significant quark contribution to hadrons.

References

1. J.C. Collins, D.E. Soper, Annu. Rev. Nucl. Part. Sci. **37**, 383 (1987)
2. J.C. Collins, D.E. Soper, G. Sterman, Adv. Ser. Direct. High Energy Phys. **5**, 1 (1988)
3. S. Albino et al., Nucl. Phys. B **725**, 181 (2005)
4. B.A. Aniehl, G. Kramer, B. Potter, Nucl. Phys. B **597**, 337 (2001)
5. D. de Florian, R. Sassot, M. Stratmann, Phys. Rev. D **76**, 074033 (2007). arXiv:0707.1506
6. J. Adams et al. (STAR Collaboration), Phys. Lett. B **637**, 161–169 (2006)
7. J. Adams et al. (STAR Collaboration), Phys. Rev. Lett. **97**, 152301 (2006)
8. B.I. Abelev et al. (STAR Collaboration), Phys. Lett. B **655**, 104 (2007)
9. J. Adams et al. (STAR Collaboration), Phys. Lett. B **616**, 8–16 (2005)
10. Y. Xu et al., arXiv:0807.4303
11. M. Beddo et al., Nucl. Instrum. Methods A **499**, 725–739 (2003)
12. S. Albino, B.A. Kniehl, G. Kramer, arXiv:0803.2768 [hep-ph]
13. I. Arsene et al. (BRAHMS Collaboration), Phys. Rev. Lett. **98**, 252001 (2007)